

Acidic Aqueous Decomposition of Thiocyanogen

Jon J. Barnett, Michael L. McKee, and David M. Stanbury*

Department of Chemistry, Auburn University, Auburn, Alabama 36849

Received May 17, 2004

The aqueous reaction of acidic Cl_2 with excess SCN^- rapidly generates a UV-absorbing intermediate identified as an equilibrium mixture of thiocyanogen, $(\text{SCN})_2$, and trithiocyanate, $(\text{SCN})_3^-$. The decomposition of this mixture can be described as $3(\text{SCN})_2 + 4\text{H}_2\text{O} \rightarrow 5\text{HSCN} + \text{H}_2\text{SO}_4 + \text{HCN}$. Under our conditions the decomposition is sufficiently slow that its kinetics can be studied using standard stopped-flow methodology. Over the pH range 0–2 the decomposition rate law is $-\text{d}[(\text{SCN})_2]/\text{d}t = (3/2)\{k_{\text{disp}}K_{\text{hyd}}^2[(\text{SCN})_2]^2/([\text{SCN}^-]^2[\text{H}^+]^2 + K_{(\text{SCN})_3^-}[\text{SCN}^-]^3[\text{H}^+]^2 + K_{\text{hyd}}[\text{SCN}^-][\text{H}^+])\}$ with $K_{(\text{SCN})_3^-} = 0.43 \pm 0.29 \text{ M}^{-1}$, $K_{\text{hyd}} = (5.66 \pm 0.77) \times 10^{-4} \text{ M}^2$, and $k_{\text{disp}} = (6.86 \pm 0.95) \times 10^4 \text{ M}^{-1} \text{ s}^{-1}$ at 25°C and $\mu = 1 \text{ M}$. The $K_{(\text{SCN})_3^-}$ and K_{hyd} terms are significant enhancements relative to one of the rate laws conventionally cited. In the proposed mechanism, $K_{(\text{SCN})_3^-}$ refers to the formation of $(\text{SCN})_3^-$ by association of SCN^- with $(\text{SCN})_2$, K_{hyd} refers to the hydrolysis of $(\text{SCN})_2$ to form HOSCN , and k_{disp} is the rate constant for the bimolecular irreversible disproportionation of HOSCN , which leads ultimately to SO_4^{2-} and HCN . Ab initio calculations support the values of $K_{(\text{SCN})_3^-}$ and K_{hyd} reported herein. The high value for k_{disp} indicates that HOSCN is a short-lived transient, while the magnitude of K_{hyd} provides information on its thermodynamic stability. These results bear on the physiological role of enzymes that catalyze the oxidation of SCN^- such as salivary peroxidase and myeloperoxidase.

Introduction

The aqueous oxidation of SCN^- has been widely studied using a variety of oxidizing agents, including HNO_3 , HNO_2 , HSO_5^- , $[\text{Ni}(\text{tacn})_2]^{3+}$, BrO_3^- , ClO_2 , and H_2O_2 .^{1–8} Early studies were focused toward the discovery of a facile method for quantitative determination of $[\text{SCN}^-]$ in solution, though many of these reactions were interesting subjects of study in and of themselves. The later discovery of the antibacterial activity of the salivary peroxidase/ H_2O_2 / SCN^- system in human saliva launched a new wave of such studies, most of which focused on the oxidation using H_2O_2 .^{9–13}

Recent work in this laboratory has focused on the kinetic analysis of the reactions of SCN^- with either H_2O_2 or ClO_2 as oxidant.^{7,8} In both of these studies an intermediate species was detected, and mechanisms were proposed in which this key intermediate was assigned to $(\text{SCN})_2$. In the ClO_2 study, analysis of the intermediate was limited by the spectral features of the species involved.⁷ In the H_2O_2 study, the $(\text{SCN})_2$ was formed in a slow reaction that occurred on a similar time scale as its further decomposition to final products.⁸ In both of these studies, the $(\text{SCN})_2$ was proposed to decompose to final products in a pseudo-second-order process.

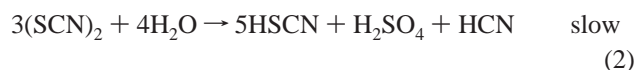
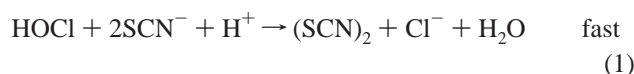
In research from other laboratories the rate law for $(\text{SCN})_2$ decomposition has been reported to be either first- or second-order in $[(\text{SCN})_2]$, and at least four distinct mechanisms have been proposed for the hydrolysis of $(\text{SCN})_2$.^{6,13–18} A common

* To whom correspondence should be addressed. E-mail: stanbdm@mail.auburn.edu.

- (1) Stedman, G.; Whincup, P. A. E. *J. Chem. Soc. A* **1969**, 1145–1148.
- (2) Hughes, M. N.; Phillips, E. D.; Stedman, G.; Whincup, P. A. E. *J. Chem. Soc. A* **1969**, 1148–1151.
- (3) Smith, R. H.; Wilson, I. R. *Aust. J. Chem.* **1966**, *19*, 1357–1363.
- (4) Smith, R. H.; Wilson, I. R. *Aust. J. Chem.* **1967**, *20*, 1353–1366.
- (5) Hung, M.-L.; Stanbury, D. M. *Inorg. Chem.* **1994**, *33*, 4062–4069.
- (6) Zhang, Y.-X.; Field, R. J. *J. Phys. Chem.* **1992**, *96*, 1224–1228.
- (7) Figlar, J. N.; Stanbury, D. M. *J. Phys. Chem. A* **1999**, *103*, 5732–5741.
- (8) Figlar, J. N.; Stanbury, D. M. *Inorg. Chem.* **2000**, *39*, 5089–5094.
- (9) Aune, T. M.; Thomas, E. L. *Eur. J. Biochem.* **1977**, *80*, 209–214.
- (10) Pruitt, K. M.; Tenovuo, J.; Andrews, R. W.; McKane, T. *Biochemistry* **1982**, *21*, 562–567.
- (11) Grisham, M. B.; Ryan, E. M. *Am. J. Physiol.* **1990**, *258*, C115–C121.

- (12) Modi, S.; Deodhar, S. S.; Behere, D. V.; Mitra, S. *Biochemistry* **1991**, *30*, 118–124.
- (13) (a) Pollock, J. R.; Goff, H. M. *Biochim. Biophys. Acta* **1992**, *1159*, 279–285. (b) Christy, A. A.; Egeberg, P. K. *Talanta* **2002**, *51*, 1049–1058.
- (14) Bjerrum, N.; Kirschner, A. K. *Dan. Vidensk. Selsk.* **1918**, *8*, 1–76.
- (15) Bjerrum, N.; Kirschner, A. *Chem. Abstr.* **1919**, *13*, 1057–1060.
- (16) Schöneshöfer, M.; Beck, G.; Henglein, A. *Ber. Bunsen-Ges.* **1970**, *74*, 1011–1015.
- (17) Wilson, I. R.; Harris, G. M. *J. Am. Chem. Soc.* **1960**, *82*, 4515–4517.

feature of the proposed decomposition mechanisms is the intermediacy of HOSCN, whose conjugate base, hypothiocyanate, has been widely cited as the active agent generated in the catalytic oxidation of SCN^- by salivary peroxidase, eosinophyl peroxidase, lactoperoxidase, and myeloperoxidase.^{11,19–27} To gain further insight into these matters, the present paper reports a detailed kinetic study of $(\text{SCN})_2$ decomposition. We use the reaction of aqueous Cl_2/HOCl with SCN^- in acidic media as a means for the rapid in situ generation of $(\text{SCN})_2$. The reaction sequence is thus



As is shown below, “ $(\text{SCN})_2$ ” under our conditions is actually an equilibrium mixture of three species. Reaction 1 as a source of $(\text{SCN})_2$ was originally suggested by Welcher and Cutrufello,²⁸ and we have published a preliminary report on the properties of the solutions thus generated.²⁹

Experimental Section

Reagents and Solutions. All solutions were prepared using water purified by passage of distilled water through either a Millipore Milli-Q Plus or a Barnstead Nanopure Infinity ultrapure water system.

HClO_4 (Fisher) and H_2SO_4 (Fisher) stock solutions were prepared by diluting the concentrated acid solutions to the desired volume. These solutions were standardized by titration to a phenolphthalein endpoint using 0.1 M NaOH solution (Fisher).

Stock solutions of $\text{LiClO}_4 \cdot 6\text{H}_2\text{O}$ (GFS) and NaCl (Fisher) were prepared by dissolution of the solid materials in water. These solutions were standardized by passage of aliquots through an acidified Dowex cation exchange column and titration of the effluents.

NaSCN stock solutions were prepared using solid NaSCN (Fisher) which had been reprecipitated from warm water. These solutions were standardized iodometrically³⁰ or colorimetrically. The iodometric method was that of Schulek.³¹ A small volume of NaSCN solution was diluted and mixed with 10 mL of 20% $\text{H}_3\text{-}$

PO_4 , Br_2 (Fisher) was then added until the solution remained slightly yellow upon mixing. Phenol solution (5%) was added to remove excess Br_2 , and this solution was allowed to sit in the dark for 20 min tightly capped. One gram of solid KI (Fisher) was then added to this mixture, and the resulting solution was then allowed to sit in the dark for 45 min tightly capped. Finally, the liberated I_2 in the solution was titrated using freshly standardized $\text{Na}_2\text{S}_2\text{O}_3$ solution.

The colorimetric method for determination of $[\text{SCN}^-]$ was based on the reaction of SCN^- with Fe^{3+} to make a complex which absorbs at 457 nm. An Fe^{3+} solution was prepared by dissolving 10 g of $\text{Fe}(\text{NO}_3)_3 \cdot 9\text{H}_2\text{O}$ (Fisher) and 5 mL of concentrated HNO_3 (Fisher) in 200 mL total volume. One milliliter of SCN^- solution was added to 5 mL of this Fe^{3+} solution, and the absorbance at 457 nm was noted after 1 min of reaction time. In order to obtain concentration data from these spectroscopic data, a calibration curve was constructed using SCN^- solutions standardized using the iodometric titration procedure described above.

Stock OCl^-/Cl^- solutions were prepared by bubbling 0.6 M carbonate-free NaOH³⁰ with UHP Cl_2 gas (Matheson). The pH of the solution was measured using a Corning rugged bulb combination pH electrode and a Corning 450 pH/ion meter. The bubbling was stopped when the pH reached a value between 11.0 and 11.5. When this solution was prepared without pH monitoring, a buildup of ClO_3^- , an excess of Cl^- , and a pH value near 4.5 resulted. If the desired pH value was overshoot during solution preparation, the pH of the resulting solution was then adjusted to approximately 11.0 to 11.5 by addition of additional NaOH. $[\text{OCl}^-]$ was determined by measurement of the solution's absorbance at $\lambda = 292$ nm, where OCl^- has $\epsilon = 350 \text{ M}^{-1} \text{ cm}^{-1}$.³²

Cl_2/HOCl solutions were prepared by mixing 7.75 mL of a solution containing the desired amount of HClO_4 and LiClO_4 with 1.25 mL of OCl^-/Cl^- solution. These solutions were combined within a 10 mL gastight syringe containing a small stir bar.³³ It is useful to define the total concentration of reducible chlorine, $[\text{Cl}_2]_{\text{tot}}$:

$$[\text{Cl}_2]_{\text{tot}} = [\text{Cl}_2] + [\text{HOCl}] \quad (3)$$

This equation arises from the following well-known hydrolysis equilibrium:



$[\text{Cl}_2]_{\text{tot}}$ can be calculated from the amount of OCl^- determined spectroscopically in the alkaline OCl^-/Cl^- solution (pH \approx 11) used in the preparation of the Cl_2/HOCl solution.

Stock CN^- solutions for use in ion chromatography experiments were prepared by dissolution of solid NaCN (Fisher) in water. The value of $[\text{CN}^-]$ in these solutions was determined by a published spectroscopic method based on the formation of the $[\text{Ni}(\text{CN})_4]^{2-}$ complex, which has a molar absorptivity of $11000 \text{ M}^{-1} \text{ cm}^{-1}$ at $\lambda = 267 \text{ nm}$.³⁴

Two eluent solutions were prepared for use in the HPLC studies. Eluent 1 was prepared by dissolution of solid KHP, potassium hydrogen phthalate (Baker & Adamson), in water to a concentration of 4 mM (pH \approx 4.3 to 4.4). Eluent 2 was prepared by dissolving 0.1 M standard NaOH solution (Fisher) and solid $\text{NaC}_7\text{H}_5\text{O}_2$, sodium benzoate (Fisher), in water to final concentrations of 4 mM

(18) Wilson, I. R.; Harris, G. M. *J. Am. Chem. Soc.* **1961**, *83*, 286–289.

(19) Pruitt, K. M.; Tenovuo, J.; Mansson-Rahemtulla, B.; Harrington, P.; Baldone, D. C. *Biochim. Biophys. Acta* **1986**, *870*, 385–391.

(20) Hoogendoorn, H.; Piessens, J. P.; Scholtes, W.; Stoddard, L. A. *Caries Res.* **1977**, *11*, 77–84.

(21) Bjoerck, L.; Claesson, O. *J. Dairy Sci.* **1980**, *63*, 919–922.

(22) Thomas, E. L.; Bates, K. P.; Jefferson, M. M. *J. Dent. Res.* **1981**, *60*, 785–796.

(23) Slungaard, A.; Mahoney, J. R. *J. Biol. Chem.* **1991**, *266*, 4903–4910.

(24) van Dalen, C. J.; Whitehouse, M. W.; Winterbourn, C. C.; Kettle, A. *J. Biochem. J.* **1997**, *327*, 487–492.

(25) Furtmüller, P. G.; Burner, U.; Obinger, C. *Biochemistry* **1998**, *37*, 17923–17930.

(26) Pruitt, K. M.; Tenovuo, J. *Biochim. Biophys. Acta* **1982**, *704*, 204–214.

(27) Tenovuo, J.; Pruitt, K. M.; Mansson-Rahemtulla, B.; Harrington, P.; Baldone, D. C. *Biochim. Biophys. Acta* **1986**, *870*, 377–384.

(28) Welcher, R. P.; Cutrufello, P. F. *J. Org. Chem.* **1972**, *37*, 4478–4479.

(29) Barnett, J. J.; Stanbury, D. M. *Inorg. Chem.* **2002**, *41*, 164–166.

(30) Kolthoff, I. M.; Sandell, E. B.; Meehan, E. J.; Bruckenstein, S. *Quantitative Chemical Analysis*, 4th ed.; Macmillan: New York, 1969; pp 849–852.

(31) Schulek, E. *Z. Anal. Chem.* **1923**, *62*, 337–342; *Chem. Abstr.* **1923**, *17*, 3465–3466.

(32) Beach, M. W.; Margerum, D. W. *Inorg. Chem.* **1990**, *29*, 1225–1232.

(33) Assefa, Z.; Stanbury, D. M. *J. Am. Chem. Soc.* **1997**, *119*, 521–530.

(34) Scoggins, M. W. *Anal. Chem.* **1972**, *44*, 1294–1296.

and 0.1 mM, respectively.³⁵ The solids were used as provided without further purification.

Other solutions for use in qualitative HPLC studies were prepared by dissolution of the solid materials in water. The solids used for these studies included NaClO₃ (J. T. Baker), NaCl (Fisher), NaClO₂ (Kodak), NaNO₂ (MCB), NaNO₃ (Fisher), Na₂SO₃ (Fisher), and NaOCN (Fluka), and all were used as provided without further purification.

Instrumental Methods. All single UV/vis spectra were collected on HP 8452a and HP 8453 diode-array spectrophotometers equipped with Brinkmann Lauda RM6 constant temperature baths in order to maintain a temperature of 25.0 (±0.1) °C.

For pH measurements, a Corning rugged-bulb combination electrode was used in combination with either a Corning 130 pH meter or a Corning 450 pH/ion meter. The filling solution of this electrode was changed from 3 M KCl to 3 M NaCl due to concerns about the solubility of KClO₄ in water.³⁶ This pH electrode was calibrated to standard buffer solutions for pH measurements on the stock OCl⁻/Cl⁻ solutions (pH ≈ 11). For pH measurements in solutions of intermediate acid strength ([H⁺] = 0.01 M to 0.1 M), a calibration curve was constructed using HClO₄ solutions of known [H⁺], controlled ionic strength (1 M (NaCl)), and controlled temperature (298 K). Above [H⁺] = 0.1 M, the value of [H⁺] was determined by titration of the acid to a phenolphthalein endpoint with standard NaOH.

Kinetic data were collected on two different instruments: (1) a Hi-Tech SF-51 stopped-flow unit equipped with a SU-40 spectrophotometer unit in the 1 cm path length configuration and a temperature control system consisting of a Hi-Tech C400 circulator and a Forma Scientific Masterline 2095 bath and circulator, and (2) an OLIS RSM-1000 rapid scanning monochromator with a USA-SF stopped-flow mixing unit with a 1.8 cm path length equipped with a Forma Scientific 2095 bath and circulator. Temperature control for both of these instruments was accurate to ±0.1 °C. For both of these instruments, data acquisition was achieved using DOS-based software from OLIS.

Note that spectrophotometry of SCN⁻ solutions requires that the wavelengths of light used for the analysis be strictly controlled. SCN⁻ undergoes photolysis below 230 nm,^{37,38} and this photolysis is more efficient at lower pH values, such as those used in the current study.³⁹ For this reason, a glass filter with a cutoff of 265 nm was used in the HP diode-array UV/vis instruments for wavelength control. In the OLIS-RSM instrument, the wavelength range used encompassed wavelengths above 250 nm. The Hi-Tech instrument is a single-wavelength instrument, and, therefore, the issue of photolytic decomposition of SCN⁻ was not a problem.

Reaction product determinations were made using a Wescan ion analyzer, model 266. The instrument was fitted with a 100 μL sample loop, a Wescan Versapump-II, and model 213A electrical conductivity and model 271 electrochemical (amperometric) detectors. The amperometric detector utilized a Ag working electrode, a Pt auxiliary electrode, and a Ag/AgCl reference electrode. This detector was operated at 0.340 V vs Ag/AgCl. The column utilized was a 25 cm resin-based anion exchange column (Wescan anion/R) with a 1.7 mL/min flow rate. Results were recorded on an Industrial Scientific OmniScribe strip chart recorder.

All uncertainties reported in this work are expressed as ± 1 standard deviation.

(35) Fritz, J. S.; Gjerde, D. T. *Ion Chromatography*, 3rd ed.; Wiley-VCH: Weinheim, FRG, 2000; pp 41–43.

(36) Weast, R. C. *CRC Handbook of Chemistry and Physics*, 66th ed.; CRC Press: Boca Raton, 1985; pp D-167–168.

(37) Dogliotti, L.; Hayon, E. *J. Phys. Chem.* **1968**, *72*, 1800–1807.

(38) Rumfeldt, R. C. *Can. J. Chem.* **1971**, *49*, 1262–1267.

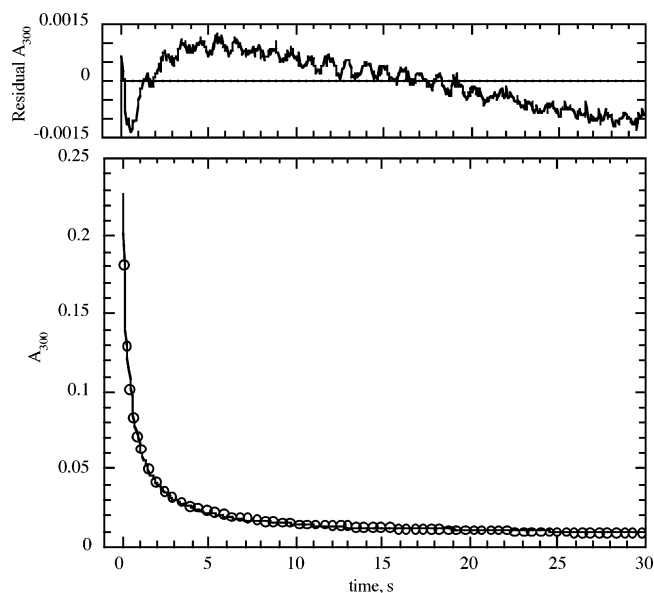


Figure 1. Homogeneous second-order fit of a single wavelength trace at $\lambda = 300$ nm. The fit was achieved using the Levenberg–Marquardt fitting routines in the OLIS software for the instrument used. The data were collected on an instrument with a path length of 1 cm and at $[\text{SCN}^-] = 25$ mM, $[\text{H}^+] = 0.1$ M, $[\text{Cl}_2]_{\text{tot}} = 1$ mM, $m = 1$ M (LiClO₄), and $T = 298$ K.

Reaction Procedures. Unless otherwise noted, all studies were performed at $T = 298$ K and $\mu = 1.0$ M (LiClO₄) and were monitored at a wavelength of 300 nm.

All studies of the [H⁺]- and [SCN⁻]-dependencies of the observed reaction kinetics were performed using the OLIS RSM-1000 with a center wavelength of 300 nm. Note that there is some question as to whether the conjugate acid of SCN⁻ is HSCN or HNCS, but in any event its pK_a has been reported to be -1.28 or -1.38.^{40,41} This means that, at the [H⁺] values utilized in the present study (pH ≥ 0), SCN⁻ can be assumed to be principally in the deprotonated form.

A study of the ionic-strength dependence of the observed reaction kinetics was performed on the Hi-Tech stopped-flow system using a set of reaction solutions in which the ionic strength was varied using LiClO₄.

A study of the temperature dependence of the observed reaction kinetics was conducted using the Hi-Tech stopped-flow system. This study was performed by first starting at the lowest temperature and then increasing the temperature of the bath surrounding the syringes containing the reaction solutions in a systematic manner. Data were collected when the bath temperature had been stable for at least 15 min.

A test for sensitivity of the observed reaction to O₂ was performed by comparison of two reactions. In the first of these reactions, the reactant solutions were prepared using Ar-sparged precursor solutions. In the other reaction, the reactant solutions were prepared using O₂-sparged precursor solutions. These reactions were studied in the Hi-Tech stopped-flow system. For the O₂-free reactions, the constant temperature bath solution surrounding the drive syringes of the apparatus was deaerated using a N₂ purge.

A Cl⁻ addition study was achieved by use of a HOCl/Cl₂ solution which had been prepared with excess added Cl⁻. Equal volumes of this solution and SCN⁻ solution were mixed using the Hi-Tech

(39) Luria, M.; Treinin, A. *J. Phys. Chem.* **1968**, *72*, 305–308.

(40) Chiang, Y.; Kresge, A. J. *Can. J. Chem.* **2000**, *78*, 1627–1628.

(41) Morgan, T. D. B.; Stedman, G.; Whincup, P. A. E. *J. Chem. Soc.* **1965**, 4813–4822.

instrument. Similarly, a SO_4^{2-} addition study was performed using a SCN^- solution containing added SO_4^{2-} .

Product anions were identified qualitatively by spiking the analyte solution with solutions containing suspected product species followed by chromatographic analysis of the resulting solutions. When quantitative results were desired, product ion concentrations were determined by peak height analysis from calibration curves of standard solutions. Product solutions for these analyses were prepared by the reaction of 2 mM $(\text{Cl}_2)_{\text{tot}}$ (as defined in eq 3) with 10 mM SCN^- in 10 mM HClO_4 using the OLIS RSM-1000 instrument as a mixer. These product solutions were diluted by a factor of either 5 or 10 before chromatographic analysis.

Computational Methods. Single wavelength fits were performed using the Levenberg–Marquardt fitting routines available within the OLIS software packages used for control of and analysis of data from the Hi-Tech and OLIS instruments. Rate constants given by the OLIS fitting routines for single wavelength traces are given with respect to the change in the absorbance value at the wavelength of interest (λ) using the following relationships:

$$-\frac{d(A_t - A_{\infty})_{\lambda}}{dt} = k_{\text{prog}}(A_t - A_{\infty})_{\lambda}^2 \quad (5a)$$

$$(A_t - A_{\infty})_{\lambda} = \frac{(A_0 - A_{\infty})_{\lambda}}{1 + k_{\text{prog}}t(A_0 - A_{\infty})_{\lambda}} \quad (5b)$$

Note that the actual fitting of the kinetic data is performed using the integrated form of the rate law shown in eq 5b. See Figure 1 for an example of a typical single wavelength trace and homogeneous second-order fit. Note that the k_{prog} values given by these fits are in terms of absorbance, which means that k_{prog} values for reactions performed at exactly the same conditions will be different when performed on instruments with different path lengths. Simple mathematical manipulations can be performed on such data to allow comparison of data from instruments with different path lengths, as will be shown herein.

All of the k_{prog} values reported herein are average values taken over at least five measurements. The data included in these average values had standard deviations less than $\pm 5\%$.

The C_s - and C_2 -symmetry structures of gas-phase $(\text{SCN})_3^-$ were optimized at the B3LYP/6-31G(d) and B3LYP/6-311+G(2d) levels.⁴² At the B3LYP/6-31G(d) level both structures were found to be minima (0 imaginary frequencies). Optimization at the B3LYP/6-311+G(2d) level resulted in very little change in the structures other than a 0.04 Å reduction in the S–S distances.

For the purpose of obtaining energetic data for species of interest, calculations were performed at either the G3B3 or G3MP2B3 level.⁴³ Solvation energies of these species in water were calculated at the CPCM/B3LYP/6-311+G(2d,p)//B3LYP/6-31G(d) level of theory.^{44,45} A correction term of 7.95 kJ/mol was used for a change of state from the gas (1 atm) to the solution phase (1 M) for aqueous species.^{46,47}

(42) Frisch, M. J.; Trucks, G. W.; Schlegel, H. B.; Scuseria, G. E.; Robb, M. A.; Cheeseman, J. R.; Zakrzewski, V. G.; Montgomery, J. A., Jr.; Stratmann, R. E.; Burant, J. C.; Dapprich, S.; Millam, J. M.; Daniels, A. D.; Kudin, K. N.; Strain, M. C.; Farkas, O.; Tomasi, J.; Barone, V.; Cossi, M.; Cammi, R.; Mennucci, B.; Pomelli, C.; Adamo, C.; Clifford, S.; Ochterski, J.; Petersson, G. A.; Ayala, P. Y.; Cui, Q.; Morokuma, K.; Malick, D. K.; Rabuck, A. D.; Raghavachari, K.; Foresman, J. B.; Cioslowski, J.; Ortiz, J. V.; Stefanov, B. B.; Liu, G.; Liashenko, A.; Piskorz, P.; Komaromi, I.; Gomperts, R.; Martin, R. L.; Fox, D. J.; Keith, T.; Al-Laham, M. A.; Peng, C. Y.; Nanayakkara, A.; Gonzalez, C.; Challacombe, M.; Gill, P. M. W.; Johnson, B.; Chen, W.; Wong, M. W.; Andres, J. L.; Head-Gordon, M.; Replogle, E. S.; Pople, J. A. *Gaussian 98*; Gaussian, Inc.: Pittsburgh, PA, 1998.

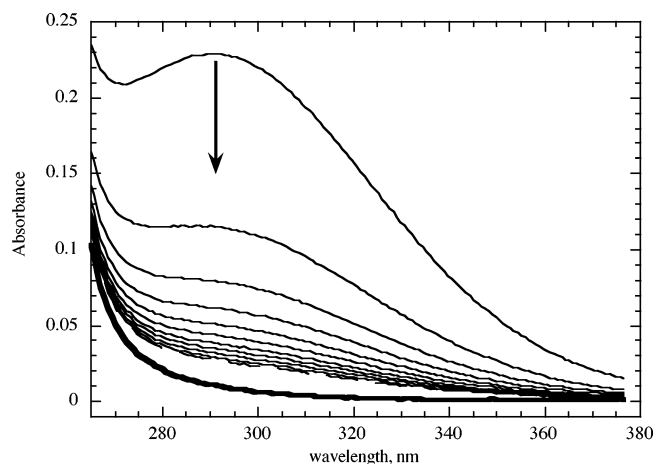


Figure 2. The change in the spectrum of the observed intermediate over time. The reaction is shown with $[\text{SCN}^-] = 25 \text{ mM}$, $[\text{H}^+] = 1 \text{ M}$, $[\text{Cl}_2]_{\text{tot}} = 1 \text{ mM}$, $\mu = 1 \text{ M}$ (LiClO_4), and $T = 298 \text{ K}$. The spectra are shown at 12 s intervals, with the exception of the final spectrum (bold line), which is shown at $t = 600 \text{ s}$.

Results

Preliminary Studies. The reaction of 1 mM $(\text{Cl}_2)_{\text{tot}}$ with 25 mM SCN^- in an aqueous solution containing 1 M HClO_4 proceeds rapidly, generating an unstable intermediate within the dead time of all stopped-flow instruments used for kinetic analysis ($\leq 3 \text{ ms}$). One interesting observation is that highly efficient mixing was necessary to obtain a full yield of the intermediate species. When the reactant solutions were mixed by hand or by other inefficient methods, a low yield resulted. When the reactant solutions were mixed using stopped-flow mixing devices, the yield was increased and was uniform over several instrument designs (Table S-1, Supporting Information). The intermediate formed shows a UV spectrum very similar to that for a species observed in the work of Figlar and Stanbury which was proposed to be $(\text{SCN})_2$.^{7,8,29} At these conditions, this intermediate decays in a slow process over a time period of 600 s. A set of spectral data from a typical kinetic study can be seen in Figure 2. Using the OLIS software supplied for the operation of the OLIS RSM-1000, the decomposition of the intermediate was found to fit well to homogeneous second-order kinetics using single wavelength traces analyzed via Levenberg–Marquardt methods. This is the same kinetic behavior observed for $(\text{SCN})_2$ in previous studies in this laboratory.^{7,8} In conjunction with the spectroscopic data collected for this intermediate species, this observation indicates that the intermediate seen in the present study is the same as the one identified as $(\text{SCN})_2$ in previous work in this laboratory.^{7,8,29}

A set of experiments was undertaken to see if the observed decomposition was sensitive to the presence or absence of O_2 . The following conditions were used in these reactions:

(43) Baboul, A. G.; Curtiss, L. A.; Redfern, P. C. *J. Chem. Phys.* **1999**, *110*, 7650–7657.

(44) Barone, V.; Cossi, M. *J. Phys. Chem. A* **1998**, *102*, 1995–2001.

(45) Barone, V.; Cossi, M.; Tomasi, J. *J. Comput. Chem.* **1998**, *19*, 404–417.

(46) Li, H.; Hains, A. W.; Everts, J. E.; Robertson, A. D.; Jensen, J. H. *J. Phys. Chem. B* **2002**, *106*, 3486–3494.

(47) Liptak, M. D.; Shields, G. C. *J. Am. Chem. Soc.* **2001**, *123*, 7314–7319.

Table 1. $[\text{Cl}_2]_{\text{tot}}$ -Dependent Kinetic Data^a

$[\text{Cl}_2]_{\text{tot}}$, mM	k_{prog} , s ⁻¹ ^b	k_{obs} , M ⁻¹ s ⁻¹ ^c
0.106	0.242	113
0.424	0.290	136
1.07	0.314	148

^a Data collected on an instrument with path length = 1.8 cm and with $[\text{SCN}^-] = 50$ mM, $[\text{H}^+] = 0.3$ M, $\mu = 1$ M (LiClO₄), and $T = 298$ K. At this value of $[\text{SCN}^-]$ and $[\text{H}^+]$, $\epsilon_{\text{eff}} = 261$ M⁻¹ cm⁻¹ from eq 11. ^b Despite appearances, k_{prog} is actually a second-order rate constant as defined in eq 5a. ^c k_{obs} values calculated using eq 14.

$[\text{H}^+] = 1$ M, $[\text{Cl}_2]_{\text{tot}} = 0.96$ mM, and $[\text{SCN}^-] = 24.4$ mM. The reaction with O₂-saturated reactant solutions showed $k_{\text{prog}} = 0.49$ s⁻¹, and the reaction with no O₂ present showed $k_{\text{prog}} = 0.60$ s⁻¹. Note that these are not first-order rate constants. As indicated by eq 5a, these are second-order rate constants given in relation to the solution's absorbance at a particular wavelength. This indicates that there is no significant effect of the presence of O₂ on the decomposition kinetics of the intermediate.

A set of reactions was performed with $[\text{Cl}_2]_{\text{tot}}$ ranging from 0.106 mM to 1.07 mM. This data set showed only a 30% rise in k_{prog} over the 10-fold increase in $[\text{Cl}_2]_{\text{tot}}$ (see Table 1), indicating that this reaction is at pseudo-second-order conditions.

Product Identification and Stoichiometry. Ion chromatographic studies allowed a detailed analysis of the anionic products of the current reaction. Using eluent 1, Cl⁻, SO₄²⁻, SCN⁻, ClO₃⁻, and ClO₄⁻ were identified as components of the product solution. All ions identified using this eluent were detected using the conductivity detector. SCN⁻, ClO₄⁻, and Cl⁻ were identified only qualitatively for various reasons. (For retention times of all ions analyzed, see Table S-2, Supporting Information.)

ClO₄⁻ is not predicted to be a product of the reaction studied and was present in high concentrations at the starting conditions. SCN⁻ was present at high concentrations at both the beginning and end of the reaction.

ClO₃⁻ was also identified as a component in some of the product solutions, but it was initially unclear whether this species was a final product of the $(\text{Cl}_2)_{\text{tot}}/\text{SCN}^-$ reaction or merely a component of one of the starting reactant solutions. Samples of the SCN⁻ and HClO₄ stock solutions were chromatographed but did not yield a ClO₃⁻ peak. The OCl⁻/Cl⁻ solution was not analyzed directly because of concerns that it might damage the column packing. Therefore, a OCl⁻/Cl⁻ solution was acidified with HClO₄, producing aqueous Cl₂, which has an absorbance at 325 nm with $\epsilon_{325} = 70$ M⁻¹ cm⁻¹.⁴⁸ This solution was sparged with N₂ until the UV/vis spectrum of the solution showed no trace of aqueous Cl₂. The resulting solution was chromatographed, revealing the presence of both Cl⁻ and ClO₃⁻. Thus, it was determined that the ClO₃⁻ seen in the product chromatogram could be entirely attributed to the amount of ClO₃⁻ in the starting Cl₂/HOCl solution. Since Cl⁻ was also present in variable concentrations, depending on the concentration of ClO₃⁻ in the starting Cl₂/HOCl reactant solution, quantitative deter-

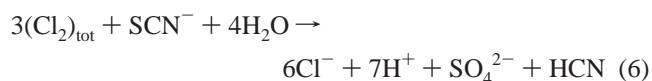
mination of the yield of Cl⁻ was not feasible. These species resulted from the preparation of the OCl⁻/Cl⁻ solution without sufficient pH control as mentioned above.

SO₄²⁻ was determined quantitatively by a peak height analysis/comparison with a calibration curve of standard SO₄²⁻ solutions. The final value of $[\text{SO}_4^{2-}]$ was found to be 0.542 (±0.070) mM when the starting $[\text{Cl}_2]_{\text{tot}}$ was 1.93 mM. It should be noted, however, that SO₃²⁻ was found to elute with the same retention time as SO₄²⁻, making it impossible to determine the exact composition of the species leading to the "SO₄²⁻" peak. It was unclear whether or not the SO₃²⁻ was converted to SO₄²⁻ inside the HPLC system, since no attempts were made to perform this analysis anaerobically and since the SO₃²⁻ was exposed to metal surfaces inside the instrument which could catalyze the oxidation to SO₄²⁻.

Several negative tests also resulted from this analysis. All of the following species were spiked into the product solution and were found not to be species present in the product chromatogram. This was based on a lack of agreement between the retention times of the added species and the retention times of species observed in chromatograms of unmodified reaction product solutions: OCN⁻, NO₂⁻, NO₃⁻, and ClO₂⁻. Note that some workers have stated that chlorate and nitrate cannot be resolved using conventional anion exchange chromatography.⁴⁹ However, the stationary phase of the Anion/R column used in the current study is functionalized with trimethylammonium groups, and the ions in question can be easily distinguished from one another using this column material and phthalate eluent.³⁵

Analysis of CN⁻ was performed with the alkaline eluent 2 in order to achieve retention of this weak acid ($\text{p}K_{\text{a}} = 9.0$ for HCN⁵⁰). The high background conductivity of the eluent yielded very unstable readings from the conductivity detector, and therefore the amperometric detector was used since it is very sensitive to CN⁻. CN⁻ was determined quantitatively by peak height analysis/comparison to a calibration curve of standard CN⁻ solutions. $[\text{CN}^-]$ was determined to be 0.627 ± 0.082 mM when the starting $[\text{Cl}_2]_{\text{tot}}$ was 2.07 mM.

The present ion chromatographic studies give $[\text{Cl}_2]_{\text{tot},0}:\text{SO}_4^{2-} \cong (3.56 \pm 0.46):1$ and $[\text{Cl}_2]_{\text{tot},0}:\text{CN}^- \cong (3.30 \pm 0.43):1$. These results are consistent with an overall stoichiometry as in



This reaction is as expected for the sum of reactions 1 and 2, the rapid generation of "(SCN)₂" and its subsequent hydrolysis. While there appear to be no prior reports on the overall stoichiometry of this reaction, the hydrolysis of (SCN)₂ has indeed been reported to proceed as shown in reaction 2.¹⁴ It has been reported previously that S(CN)₂ is a product of (SCN)₂ hydrolysis.¹⁸ S(CN)₂ apparently arises through attack of HCN on (SCN)₂ under conditions of high

(48) Wang, T. X.; Kelly, M. D.; Cooper, J. N.; Beckwith, R. C.; Margerum, D. W. *Inorg. Chem.* **1994**, *33*, 5872–5878.

(49) Weiss, J. *Ion Chromatography*, 2nd ed.; VCH: New York, 1995; p 255.

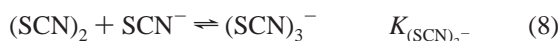
(50) Cotton, A. L.; Wilkinson, G. *Advanced Inorganic Chemistry*, 4th ed.; John Wiley & Sons: New York, 1980; p 369.

$[(\text{SCN})_2]$ and an excess of oxidant. Under the conditions of the present work, with excess SCN^- , any $\text{S}(\text{CN})_2$ produced would be expected to react with SCN^- to form $(\text{SCN})_2$ and thus lead to the observed stoichiometry (eq 6). It has also been suggested that “ H_2SO_3 ” is a product of $(\text{SCN})_2$ hydrolysis, but we find no evidence that this species was actually detected in the prior studies.^{4,6,18}

[SCN^-] Dependence of $(A_0)_{300}$. The initial absorbance at $\lambda = 300$ nm, $(A_0)_{300}$, is highly dependent on $[\text{SCN}^-]$.²⁹ Due to the observed dependence on $[\text{SCN}^-]$ and $[\text{H}^+]$, it is useful to define a variable ϵ_{eff} , which is the effective molar absorptivity for the intermediate at $\lambda = 300$ nm and at a given $[\text{SCN}^-]$:

$$\epsilon_{\text{eff}} = \frac{(A_0 - A_\infty)_{300}}{[\text{Cl}_2]_{\text{tot}} l} \quad (7)$$

Equation 7 is based on the assumption of quantitative conversion of $(\text{Cl}_2)_{\text{tot}}$ to the intermediate. It is assumed that the intermediate participates in two rapid equilibria:



The further assumption is made that the absorbance arises from $(\text{SCN})_2$ and $(\text{SCN})_3^-$ as in

$$A_{\text{tot}} = A_{(\text{SCN})_2} + A_{(\text{SCN})_3^-} \\ (\epsilon_{(\text{SCN})_2}[(\text{SCN})_2] + \epsilon_{(\text{SCN})_3^-}[(\text{SCN})_3^-])l \quad (10)$$

which leads to eq 11:

$$\epsilon_{\text{eff}} = \frac{\epsilon_{(\text{SCN})_2} + \epsilon_{(\text{SCN})_3^-} K_{(\text{SCN})_3^-} [\text{SCN}^-]}{1 + K_{(\text{SCN})_3^-} [\text{SCN}^-] + \frac{K_{\text{hyd}}}{[\text{SCN}^-][\text{H}^+]}} \quad (11)$$

As we reported previously, the spectra are strongly influenced by the formation of $(\text{SCN})_3^-$, although the low value for $K_{(\text{SCN})_3^-}$ makes it difficult to resolve the individual values of $\epsilon_{(\text{SCN})_3^-}$ and $K_{(\text{SCN})_3^-}$.²⁹ The formation of $(\text{SCN})_3^-$ can account for the differences in prior literature reports of the spectrum of $(\text{SCN})_2$.^{1,7,51} Equation 11 differs from that used in our prior report through the inclusion of the K_{hyd} term;²⁹ this modification is made in order to achieve consistency with the kinetic data reported below. From analysis of the previously reported spectroscopic data²⁹ using eq 11 the following parameters are obtained: $\epsilon_{(\text{SCN})_2} = 71 \pm 12 \text{ M}^{-1} \text{ cm}^{-1}$, $K_{(\text{SCN})_3^-} = 0.43 \pm 0.29 \text{ M}^{-1}$, $\epsilon_{(\text{SCN})_3^-} = (9.5 \pm 6.6) \times 10^3 \text{ M}^{-1} \text{ cm}^{-1}$, and $K_{\text{hyd}} = (5.4 \pm 1.9) \times 10^{-4} \text{ M}^2$. Within the indicated uncertainties the values for $\epsilon_{(\text{SCN})_2}$, $K_{(\text{SCN})_3^-}$, and $\epsilon_{(\text{SCN})_3^-}$ are in agreement with our prior report, although the inclusion of the K_{hyd} term has led to significant increases in the uncertainties of these quantities. The large uncertainties arise from strong correlation between the parameters and difficulties in attaining conditions where the equilibria are substan-

tially shifted toward products. In principle, the uncertainties relating to $(\text{SCN})_3^-$ could be reduced by collecting data at higher $[\text{SCN}^-]$, while those relating to HOSCN could be improved by use of data at higher pH. However, increasing $[\text{SCN}^-]$ beyond the current values is ruled out by the constraints of the ionic strength (1.0 M). Experiments at higher pH are also ruled out, in this case by the high reaction rates at high pH that lead to significant loss of the intermediate within the dead time of the stopped-flow instrument. Despite the large uncertainties it is still possible to use these parameters with eq 11 to calculate quite accurate values of ϵ_{eff} . As is shown below, accurate kinetic data can be obtained at higher pH than is possible for accurate A_0 values, and thus we consider the value for K_{hyd} obtained from kinetic data to be more reliable than the one given above.

Decomposition Kinetics. It is convenient to obtain ϵ_{eff} values from eq 11 and the parameters given above rather than to use directly obtained ϵ_{eff} values because, at many of the reaction conditions employed herein, a significant amount of decomposition of the observed intermediate occurs within the dead time of the instruments used. The calculated ϵ_{eff} value can be used to extract molar pseudo-second-order rate constants from the k_{prog} values given from the OLIS fits of the kinetic data. An observed rate constant, k_{obs} , can be defined as follows:

$$-\frac{d[(\text{SCN})_2]_{\text{tot}}}{dt} = k_{\text{obs}}[(\text{SCN})_2]_{\text{tot}}^2 \quad (12)$$

where $[(\text{SCN})_2]_{\text{tot}}$ is defined as

$$[(\text{SCN})_2]_{\text{tot}} = [(\text{SCN})_2] + [(\text{SCN})_3^-] + [\text{HOSCN}] \quad (13)$$

Equations 11–13, taken with eq 5a, give the following relationship:

$$k_{\text{obs}} = k_{\text{prog}} l \epsilon_{\text{eff}} \quad (14)$$

Since the calculation of k_{obs} takes into account the path length of the instrument used, k_{obs} values from instruments with different path lengths can be compared directly as long as the reactions to be compared are carried out at the same conditions.

[SCN^-] Dependence. A series of studies was performed in which $[\text{SCN}^-]$ was varied from 7.6 mM to 101 mM at $[\text{H}^+] = 0.5 \text{ M}$ and $[\text{Cl}_2]_{\text{tot}} = 1 \text{ mM}$. Pseudo-second-order rate constants were determined using the OLIS fitting routines as described above (Table S-3, Supporting Information). Figure 3 shows a plot of the collected data as $\log k_{\text{obs}}$ vs $\log [\text{SCN}^-]$. The resulting linear plot has a slope of -1.66 , significantly greater than -2 .

[H^+] Dependence. A series of experiments was performed in which $[\text{HClO}_4]$ was varied from 0.0116 M to 1.00 M with $[\text{SCN}^-] = 25 \text{ mM}$ and $[\text{Cl}_2]_{\text{tot}} = 1.00 \text{ mM}$. Above 0.1 M H^+ , $[\text{H}^+]$ was calculated from dilutions of a standardized stock solution of HClO_4 , and for the acid concentrations from 0.01 M to 0.1 M, the $[\text{H}^+]$ values were determined by measurement via the pH meter/electrode combination described earlier. Figure 4 shows a plot of these data as \log

(51) Dolbear, G. E.; Taube, H. *Inorg. Chem.* **1967**, *6*, 60–64.

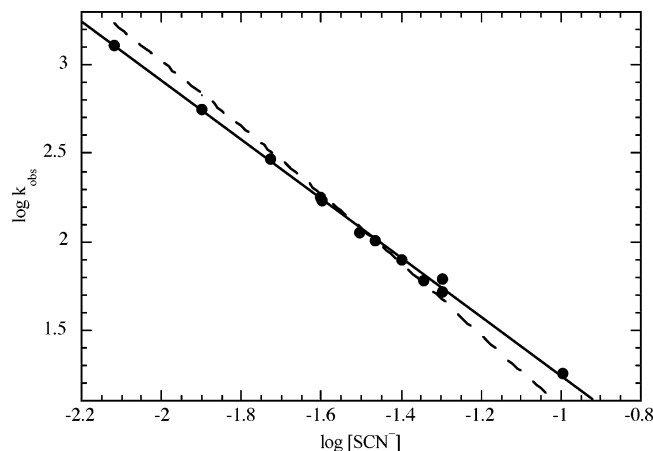


Figure 3. Variation of the observed pseudo-second-order rate constant with $[\text{SCN}^-]$. Data collected on an instrument with a 1.8 cm path length and at $[\text{H}^+] = 0.5 \text{ M}$, $[\text{Cl}_2]_{\text{tot}} = 1 \text{ mM}$, $m = 1 \text{ M}$ (LiClO_4), and $T = 298 \text{ K}$. The solid line represents a linear fit of the data. The slope of this line is -1.66 . The dashed line represents the best fit of the data to eq 20.

k_{obs} vs $\log [\text{H}^+]$ (data in Table S-4, Supporting Information). The resulting plot is linear above 0.05 M H^+ , but becomes significantly nonlinear at lower acidity. The slope in the linear region is -1.79 and is significantly greater than -2 .

Temperature Dependence. A series of reactions were performed with $[\text{H}^+] = 0.300 \text{ M}$, $[\text{Cl}_2]_{\text{tot}} = 1.00 \text{ mM}$, and $[\text{SCN}^-] = 25.2 \text{ mM}$ in which the temperature was varied from 284.9 K to 317.3 K . Note that k_{obs} values (Table S-5, Supporting Information) were calculated using ϵ_{eff} values that were determined at each temperature using eq 7; the use of eq 11 with the parameters given above instead of eq 7 would lead to errors because both $K_{(\text{SCN})_3^-}$ and K_{hyd} should shift with changing temperature. In order to compare these data with those of prior workers we have used their approximate rate law to calculate values of k' .^{1,7,8,14,15} This rate law is

$$\frac{-d[(\text{SCN})_2]_{\text{tot}}}{dt} = \frac{k'[(\text{SCN})_2]_{\text{tot}}^2}{[\text{H}^+]^2[\text{SCN}^-]^2} \quad (15)$$

and thus

$$k' = k_{\text{obs}}[\text{SCN}^-]^2[\text{H}^+]^2 \quad (16)$$

As suggested by the Eyring equation, a plot of $\ln(k'/T)$ as a function of $1/T$ is shown in Figure 5. The plot is linear with a slope of -6830 K and an intercept of 13.8 . We do not derive activation parameters from this plot because, as is discussed below, eqs 15 and 16 are not the true rate law.

Effect of Ionic Strength. A series of experiments were performed on a set of reaction solutions in which ionic strength, μ , was varied from 0.128 M to 1.20 M using LiClO_4 . In these studies, $[\text{SCN}^-] = 25.5 \text{ mM}$, $[\text{H}^+] = 0.102 \text{ M}$, and $[\text{Cl}_2]_{\text{tot}} = 0.483 \text{ mM}$. Note that ϵ_{eff} values were determined at each ionic strength using eq 7 rather than eq 11 because the latter contains both $K_{(\text{SCN})_3^-}$ and K_{hyd} . Though $K_{(\text{SCN})_3^-}$ is not expected to shift substantially with changing ionic strength, a significant shift could be expected in K_{hyd} due to the differing numbers of ionic species on each side of the equilibrium expression shown in reaction 9. Therefore, μ -dependent ϵ_{eff} values must be used in eq 14 for the

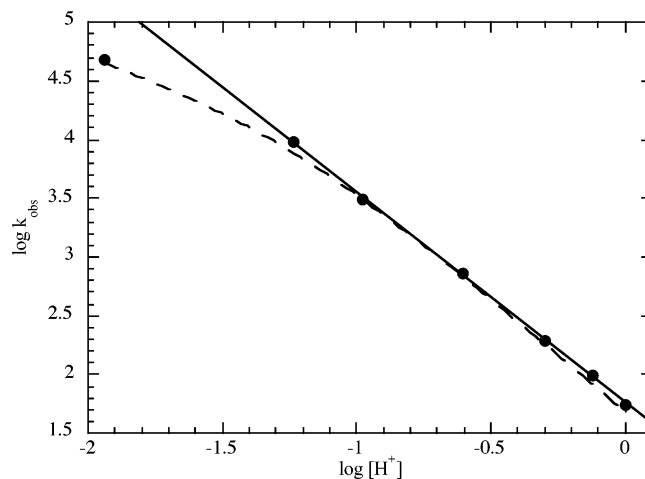


Figure 4. Variation of the observed pseudo-second-order rate constant with $[\text{H}^+]$. Data collected on an instrument with a 1.8 cm path length and at $[\text{SCN}^-] = 25 \text{ mM}$, $[\text{Cl}_2]_{\text{tot}} = 1 \text{ mM}$, $\mu = 1 \text{ M}$ (LiClO_4), and $T = 298 \text{ K}$. The solid line represents the best linear fit of the data with the lowest acid data point not included. The slope of this line is -1.79 . The dashed line represents the best fit of the data to eq 20.

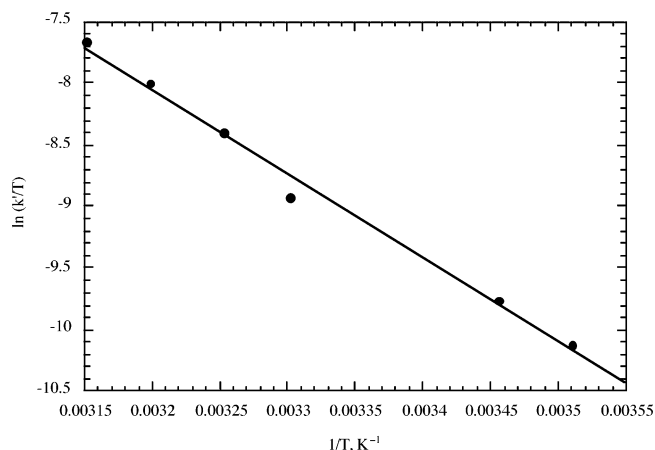


Figure 5. Variation of the value of k' with T . Data collected on an instrument with a 1 cm path length and at $[\text{SCN}^-] = 25.2 \text{ mM}$, $[\text{H}^+] = 0.300 \text{ M}$, $[\text{Cl}_2]_{\text{tot}} = 0.975 \text{ mM}$, and $\mu = 1.00 \text{ M}$ (LiClO_4). Slope = -6830 K , and intercept = 13.8 .

calculation of k_{obs} values. A plot of these k' data can be seen in Figure 6 (data in Table S-6, Supporting Information). The variables plotted in this figure are those recommended for the Brønsted–Debye–Hückel equation.⁵²

Effect of Possible Products. Two studies were conducted in which possible final products of the reaction of Cl_2 with SCN^- were added to reaction solutions to see what effect, if any, they would have on the decomposition of the observed intermediate if present in the reaction medium. Species for use as possible products in this set of studies were those predicted in the work of earlier researchers.^{14,18} Data from these experiments can be seen in Table 2.

One expected product of the reaction is Cl^- . A reaction was performed with added $[\text{Cl}^-] = 100 \text{ mM}$, $[\text{H}^+] = 0.5 \text{ M}$, $[\text{Cl}_2]_{\text{tot}} = 1.02 \text{ mM}$, and $[\text{SCN}^-] = 25.13 \text{ mM}$. The value of k_{obs} for the decomposition of the intermediate with the Cl^- present is $384 \text{ M}^{-1} \text{ s}^{-1}$ compared to the value of 309

(52) Espenson, J. H. *Chemical Kinetics and Reaction Mechanisms*, 2nd ed.; McGraw-Hill: New York, 1995; pp 71–76.

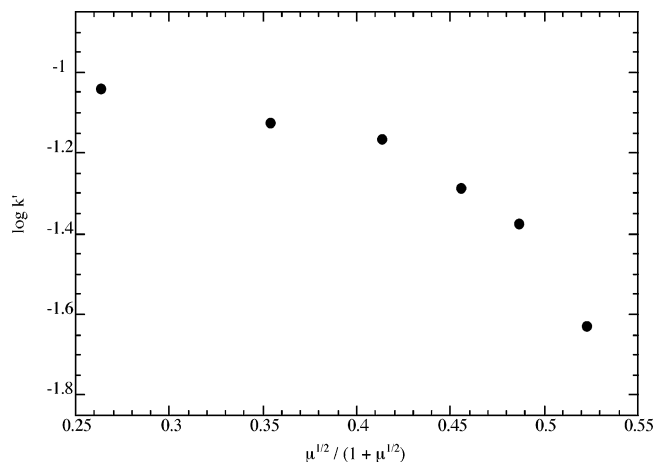


Figure 6. Dependence of k' on μ . Data collected on an instrument with a 1 cm path length and at $[\text{SCN}^-] = 25.5 \text{ mM}$, $[\text{H}^+] = 0.102 \text{ M}$, $[\text{Cl}_2]_{\text{tot}} = 0.483 \text{ mM}$, and $T = 298 \text{ K}$.

Table 2. Dependence of Observed Kinetics on Added Species^a

$[\text{SO}_4^{2-}]$ added, mM	$[\text{Cl}^-]$ added, mM	k_{prog} , s^{-1} ^b	k_{obs} , $\text{M}^{-1} \text{ s}^{-1}$ ^c
0	0	1.88	309
0	100	2.34	384
99.9	0	3.20	526

^a Data collected on an instrument with path length = 1 cm and with $[\text{SCN}^-] = 25 \text{ mM}$, $[\text{H}^+] = 0.50 \text{ M}$, $[\text{Cl}_2]_{\text{tot}} = 1 \text{ mM}$, and $\mu = 1 \text{ M}$ (LiClO_4). At this value of $[\text{SCN}^-]$ and $[\text{H}^+]$, $\epsilon_{\text{eff}} = 164 \text{ M}^{-1} \text{ cm}^{-1}$, as calculated using eq 11. ^b Despite appearances, k_{prog} is actually a second-order rate constant as defined in eq 5a. ^c k_{obs} values calculated using eq 14.

$\text{M}^{-1} \text{ s}^{-1}$ for a reaction at the same conditions with no added Cl^- . This is an increase of only $\approx 25\%$ in the value of k_{obs} with Cl^- present at ≈ 50 times the concentration expected in the final product solution of this reaction. Thus, there appears to be no significant effect of Cl^- on the observed kinetics.

One identified product of this reaction is SO_4^{2-} . A set of reactions was performed with 100 mM added SO_4^{2-} at $[\text{H}^+] = 0.5 \text{ M}$, $[\text{Cl}_2]_{\text{tot}} = 1.02 \text{ mM}$, $[\text{SCN}^-] = 25.13 \text{ mM}$, $\mu = 1 \text{ M}$ (LiClO_4), and $T = 298 \text{ K}$. Note that H_2SO_4 was used as the source of SO_4^{2-} in this set of experiments. The second $\text{p}K_{\text{a}}$ value for H_2SO_4 is 1.08 at $\mu = 1 \text{ M}$ and $T = 298 \text{ K}$.⁵³ These reactions were performed at $\text{pH} \approx 0.3$. For ionic strength and $[\text{H}^+]$ calculations, the SO_4^{2-} source was treated as a 1:1 electrolyte, though this was not necessarily the case since approximately 14% of the HSO_4^- was actually in the form of SO_4^{2-} at these conditions. Thus, μ and $[\text{H}^+]$ values calculated in this manner were slightly lower than the true values present in these reaction solutions. The k_{obs} value with no added SO_4^{2-} is $309 \text{ M}^{-1} \text{ s}^{-1}$, and the observed value with the added SO_4^{2-} is $526 \text{ M}^{-1} \text{ s}^{-1}$. This is a $\approx 70\%$ increase in the value of k_{obs} at $[\text{SO}_4^{2-}] \approx 300$ times the amount expected in the final product of this solution. Thus, there appears to be only a modest effect of SO_4^{2-} on the decomposition kinetics of the intermediate when $[\text{SO}_4^{2-}]$ is very high.

Discussion

The reaction of the HOCl/Cl_2 solution with SCN^- solution produces an intermediate in a process that is too rapid for study by techniques available within this laboratory. In Figure

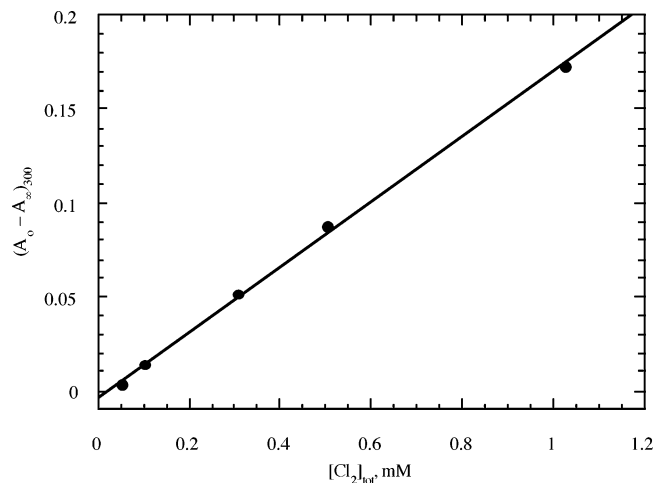


Figure 7. The variation of the absorbance at $l = 300 \text{ nm}$ with $[\text{Cl}_2]_{\text{tot}}$. Data collected using an instrument with a path length of 1 cm and at $[\text{SCN}^-] = 25 \text{ mM}$, $[\text{H}^+] = 1 \text{ M}$, $m = 1.02 \text{ M}$ (LiClO_4), and $T = 298 \text{ K}$. The linear fit of the data has a slope of 173 M^{-1} . At these conditions, eq 11 predicts $\epsilon_{\text{eff}} = 168 \text{ M}^{-1} \text{ cm}^{-1}$.

7, it can be seen that the value of $(A_0 - A_{\infty})_{300}$ varies directly with the value of $[\text{Cl}_2]_{\text{tot},0}$ with an intercept that is nearly zero. This indicates that the absorbing intermediate is produced in direct proportion to the starting concentration of HOCl/Cl_2 , as should be the case if $(\text{SCN})_2$ were being formed from the reaction with SCN^- . The slope of the plot in Figure 7 matches quite well the value of ϵ_{eff} at the $[\text{SCN}^-]$ in those solutions. The intermediate formed shows a spectrum that matches well the shape of the aqueous spectrum predicted in the work of Figlar and Stanbury^{7,8} and the one reported in the work of Bacon and Irwin for $(\text{SCN})_2$ in CCl_4 ,⁵⁴ although the value of $\epsilon_{(\text{SCN})_2}$ calculated in the current work is a factor of 2 less than the values determined in these earlier investigations. However, it should be noted that the value reported by Figlar and Stanbury is actually ϵ_{eff} and not $\epsilon_{(\text{SCN})_2}$. At the values of $[\text{SCN}^-]$ and $[\text{H}^+]$ used in that earlier study, ϵ_{eff} is predicted to be $167 \text{ M}^{-1} \text{ cm}^{-1}$ at $\lambda = 300 \text{ nm}$ using eq 11. This calculated value for ϵ_{eff} is in good agreement with $159 \text{ M}^{-1} \text{ cm}^{-1}$, which is the value reported at $\lambda = 288 \text{ nm}$ in the work of Figlar and Stanbury.⁷ The difference between the currently obtained value and the one determined in CCl_4 should not be a result of the formation of $(\text{SCN})_3^-$.⁵⁴ The spectra for the halogens have been observed to show decreases in ϵ and shifts in the wavelength of maximum absorbance with a change of solvent from CCl_4 to H_2O (Table 3).

The intermediate hydrolyzes relatively slowly in acidic aqueous solutions, enabling a detailed study of this process. The $[\text{H}^+]$ and $[\text{SCN}^-]$ dependence studies performed support the empirical rate law:

$$\frac{-d[(\text{SCN})_2]_{\text{tot}}}{dt} = \frac{k [(\text{SCN})_2]_{\text{tot}}^2}{[\text{H}^+]^{1.79} [\text{SCN}^-]^{1.66}} \quad (17)$$

(53) Smith, R. M.; Martell, A. E.; Motekaitis, R. J. *NIST Critically Selected Stability Constants of Metal Complexes Database, 4.0*; U.S. Department of Commerce: Gaithersburg, MD, 1997.

(54) Bacon, R. G. R.; Irwin, R. S. *J. Chem. Soc.* **1958**, 778–784.

Table 3. Changes in the Absorbance Spectrum of X₂ with Changing Solvent

X ₂	solvent	λ, nm	ε _λ , M ⁻¹ cm ⁻¹	ref
I ₂	H ₂ O	460	746	66
I ₂	CCl ₄	517	918	67
Br ₂	H ₂ O	390	175	68
Br ₂	CCl ₄	417	203	67

Table 4. Proposed Mechanism^a

reaction	step
HOCl + Cl ⁻ + H ⁺ ⇌ Cl ₂ + H ₂ O	(M1)
HOCl + SCN ⁻ + H ⁺ → ClSCN + H ₂ O	(M2)
Cl ₂ + SCN ⁻ → ClSCN + Cl ⁻	(M3)
ClSCN + SCN ⁻ → (SCN) ₂ + Cl ⁻	(M4)
(SCN) ₂ + SCN ⁻ ⇌ (SCN) ₃ ⁻	$K_{(\text{SCN})_3^-}$ (M5)
(SCN) ₂ + H ₂ O ⇌ HOSCN + SCN ⁻ + H ⁺	K_{hyd} (M6)
2HOSCN → HO ₂ SCN + SCN ⁻ + H ⁺	k_{disp} (M7)
2HO ₂ SCN → O ₃ SCN ⁻ + HOSCN + H ⁺	k'' (M8)
O ₃ SCN ⁻ + H ₂ O → SO ₄ ²⁻ + HCN + H ⁺	(M9)

^a Steps M1 to M4 are assumed to be very rapid due to the appearance of (SCN)₂ within the dead time of all of the instruments used. Step M5 is proposed to account for the rising (A₀)₃₀₀ with rising [SCN⁻]. Steps M6 to M9 are proposed on the basis of analogous halogen chemistry.

This disagrees significantly with the observations of Bjerrum and Kirschner, and with those of subsequent workers, who noted the second-order decay of (SCN)₂ but also an inverse second-order dependence on both [H⁺] and [SCN⁻] (eq 15).^{1,7,8,14,15} It should be noted that the work of Bjerrum and Kirschner only covered a range of [H⁺] from 0.4 M to 1 M and a range of [SCN⁻] from 0.08 M to 0.2 M.^{14,15} Equation 17 disagrees with the findings of Schöneshöfer et al., who reported a first-order rate law for this process;¹⁶ the origin of this disagreement is discussed below.

The mechanism shown in Table 4 is proposed for the present reaction system. Steps M2 to M4 are very rapid, coming to completion in less than 3 ms, which is the dead-time limit of the instruments used in this study. Steps M6 to M8 are likely steps which are based on analogous halogen chemistry and which have been proposed in previous studies.^{1,7,8} Halogen equivalents of step M7 have been reported for both HOI⁵⁵ and HOBr.⁵⁶ In each of these reports a reaction step is proposed in which 2 HOX molecules disproportionate to give HO₂X, X⁻, and H⁺. Also, both of these reactions are reported to have rate laws of the general form rate = $k_{\text{obs}} [\text{HOX}]^2$. Step M9 has halogen equivalents in the hydrolysis reaction of XSO₃⁻ to give X⁻, H⁺, and SO₄²⁻, where X = F, Cl, Br, or I.^{56–59}

The equilibrium shown in step M5 is proposed on the basis of the variation of (A₀)₃₀₀ with [SCN⁻]. Since a variation of similar magnitude is not produced by a similar change in [H⁺], the observed change cannot be due to a shift in the hydrolysis equilibrium for (SCN)₂, shown in step M6 of the proposed mechanism.²⁹ Therefore, there is some process involving SCN⁻ and (SCN)₂ which leads to a higher value

Table 5. Values Reported for K_{hyd} for Different X₂ Species

X ₂	K_{hyd} , M ²	ref
Cl ₂	3.35×10^{-4} ^b	69
BrCl ^a	1.3×10^{-4} ^b	68
Br ₂	6.2×10^{-9} ^b	70
I ₂	4.3×10^{-13}	71
(SCN) ₂	5.4×10^{-4} ^b	this work ^c
(SCN) ₂	5.66×10^{-4} ^b	this work ^d

^a Value reported for the hydrolysis of the interhalogen compound indicated, yielding HOBr. ^b Values reported at $T = 298$ K and $\mu = 1$ M. ^c K_{hyd} calculated from ϵ_{eff} values using eq 11. ^d K_{hyd} calculated from k_{obs} values using eq 20.

for (A₀)₃₀₀. Also, the shift of the wavelength of maximum absorbance, λ_{max} , to slightly higher λ with increasing [SCN⁻] seems to indicate the presence of at least two absorbing species.²⁹ The formation of trithiocyanate, (SCN)₃⁻, is proposed to account for these observations. Steps M7–M9 of the proposed mechanism describe the decomposition of (SCN)₂/(SCN)₃⁻/HOSCN to final products, and in conjunction with the prior steps lead to the overall observed stoichiometry shown in eq 6.

Several mechanisms have been proposed for the aqueous decomposition of (SCN)₂. One might envision a scheme such as that proposed in the work of Wilson and Harris which involves the hydrolysis of HO₂SCN to form a S(IV) species such as SO₃²⁻, HSO₃⁻, or SO₂ as an intermediate, the latter of which is more likely in acidic conditions.¹⁸ Several previous studies have reported on the reactions of halogens with S(IV) species in aqueous solution. HOBr has been shown to react with SO₃²⁻ with a second-order rate constant of $(5 \pm 1) \times 10^9$ M⁻¹ s⁻¹.⁵⁶ This reaction was observed to occur more rapidly at the lower pH values covered in that study, though it is worth noting that the reactions were all performed at or above pH 8. In a separate study by the same group, I₂ was reported to react with SO₃²⁻ and HSO₃⁻ with second-order rate constants of 3.1×10^9 M⁻¹ s⁻¹ and 1.7×10^9 M⁻¹ s⁻¹, respectively.⁵⁸ This work was performed in the pH range from 4.1 to 6.6. Similarly, we expect that (SCN)₂ or HOSCN would react with HSO₃⁻ or related species if such species were present as intermediates in this reaction. However, a reaction could be envisioned which is faster than the reaction of both (SCN)₂ and HOSCN with HSO₃⁻ and which yields SO₄²⁻ from SO₃²⁻. There exists no method for ruling out such a process in this system based on analysis of the kinetic data collected in the present study. However, very preliminary data on the addition of SO₂ to solutions of (SCN)₂ seem to indicate a possible reaction of (SCN)₂ with the added species to give a new absorbing species not previously seen in this study.⁶⁰ These data were collected by hand-mixing of the solutions of interest, and are, therefore, not of very high quality. However, this study does seem to imply that the proposed SO₃²⁻-producing pathway is not active in the present system. The SO₄²⁻ and Cl⁻ addition studies from the present work are consistent with the mechanism proposed in Table 4 above, as neither of these proposed final products show significant interference with the decomposition kinetics of the intermediate even at

(55) Urbansky, E. T.; Cooper, B. T.; Margerum, D. W. *Inorg. Chem.* **1997**, *36*, 1338–1344.

(56) Troy, R. C.; Margerum, D. W. *Inorg. Chem.* **1991**, *30*, 3538–3543.

(57) Yiin, B. S.; Margerum, D. W. *Inorg. Chem.* **1988**, *27*, 1670–1672.

(58) Yiin, B. S.; Margerum, D. W. *Inorg. Chem.* **1990**, *29*, 1559–1564.

(59) Jones, M. M.; Lockhart, W. L. *J. Inorg. Nucl. Chem.* **1968**, *30*, 1237–1243.

(60) Barnett, J. J. Ph.D. Dissertation, Auburn University, 2002.

concentrations far beyond which they would exist under normal reaction conditions.

The following rate law can be derived for the decomposition of $(\text{SCN})_2$ based on the mechanism listed in Table 4 and making the following assumptions: (1) Step M7 of the proposed mechanism is the rate-determining step, and (2) the steady-state approximation is assumed for $[\text{HO}_2\text{SCN}]$.

$$\frac{-d[(\text{SCN})_2]}{dt} = \frac{3}{2} \times \left(\frac{k_{\text{disp}}K_{\text{hyd}}^2[(\text{SCN})_2]^2}{[\text{SCN}^-]^2[\text{H}^+]^2 + K_{(\text{SCN})_3^-}[\text{SCN}^-]^3[\text{H}^+]^2 + K_{\text{hyd}}[\text{SCN}^-][\text{H}^+]} \right) \quad (18a)$$

$$= \frac{3k_{\text{disp}}K_{\text{hyd}}^2[(\text{SCN})_2]^2}{2[\text{H}^+]^2[\text{SCN}^-]^2 \left(1 + K_{(\text{SCN})_3^-}[\text{SCN}^-] + \frac{K_{\text{hyd}}}{[\text{SCN}^-][\text{H}^+]} \right)} \quad (18b)$$

Alternatively, as is shown in the Supporting Information and in terms of $[(\text{SCN})_2]_{\text{tot}}$ the rate law can be written as

$$\frac{-d[(\text{SCN})_2]_{\text{tot}}}{dt} = \frac{3}{2} \left(\frac{k_{\text{disp}}K_{\text{hyd}}^2[(\text{SCN})_2]_{\text{tot}}^2}{[\text{H}^+]^2[\text{SCN}^-]^2} \right) \times \left(1 + K_{(\text{SCN})_3^-}[\text{SCN}^-] + \frac{K_{\text{hyd}}}{[\text{H}^+][\text{SCN}^-]} \right)^{-2} \quad (19)$$

Comparison with eq 9 then leads to

$$k_{\text{obs}} = \frac{3k_{\text{disp}}K_{\text{hyd}}^2}{2[\text{H}^+]^2[\text{SCN}^-]^2} \times \left(1 + K_{(\text{SCN})_3^-}[\text{SCN}^-] + \frac{K_{\text{hyd}}}{[\text{SCN}^-][\text{H}^+]} \right)^{-2} \quad (20)$$

The k_{obs} data collected at constant temperature and ionic strength were fit to this equation using a nonlinear least-squares program.⁶¹ In this fit of the data, the value of $K_{(\text{SCN})_3^-}$ was held constant at 0.43 M^{-1} , which is the value determined from the fit of ϵ_{eff} using eq 11. The reason for holding this value constant is that all of the kinetic data presented in the present work were collected at relatively low values of $[\text{SCN}^-]$. At these conditions, $K_{(\text{SCN})_3^-}$ cannot be resolved from the kinetic data. Therefore, the value obtained from the analysis of the ϵ_{eff} data over a larger range of $[\text{SCN}^-]$ values was used for the fitting of the kinetic data. The quality of the fit is demonstrated by the dashed lines in Figures 3 and 4. Note in particular the good agreement of the data at low $[\text{H}^+]$ in Figure 4. K_{hyd} was found to be $(5.66 \pm 0.77) \times 10^{-4} \text{ M}^2$, and the quantity $k_{\text{disp}}K_{\text{hyd}}^2$ was found to be $(2.20 \pm 0.10) \times 10^{-2} \text{ M}^3 \text{ s}^{-1}$. These values give $k_{\text{disp}} = (6.86 \pm 0.95) \times 10^4 \text{ M}^{-1} \text{ s}^{-1}$. The value of K_{hyd} calculated from the k_{obs} data compares excellently to $(5.4 \pm 1.9) \times 10^{-4} \text{ M}^2$, which is calculated from the ϵ_{eff} data using eq 11. As is noted above, this value for K_{hyd} is considered to be more accurate than

the one derived from the initial absorbance data because the kinetic data were obtained at higher pH. Further support for this determination of K_{hyd} is obtained from ab initio calculations as described below. As is shown in Table 5, the values of K_{hyd} for the halogens bracket the value of K_{hyd} for $(\text{SCN})_2$ seen in the current study.

Schöneshöfer et al., published a study on the aqueous decomposition of $(\text{SCN})_2$ produced using pulse radiolysis.¹⁶ In that work, a value of $K_{\text{hyd}} = 3 \times 10^{-11} \text{ M}^2$ was determined, which differs by 7 orders of magnitude from the currently reported value. Also, the rate law observed in this work was first-order in $[(\text{SCN})_2]$ and inverse first-order with respect to both $[\text{H}^+]$ and $[\text{SCN}^-]$. The kinetic and equilibrium data reported in Schöneshöfer's study conflict with the observations of several prior and subsequent researchers on this system.^{1,7,8,14,15,29} It seems likely that, since Schöneshöfer et al. were measuring their kinetic data via conductivity measurements, they might have been observing the progress of some other step or steps in the reaction mechanism from the ones which can be probed using UV spectroscopic techniques.¹⁶ One likely candidate is the hydrolysis of $\text{HO}_3\text{-SCN}$ proposed as step M9 of the mechanism in Table 4.

We also note that Zhang and Field reported on the hydrolysis of $(\text{SCN})_2$ as part of their study of the oxidation of SCN^- by BrO_3^- .⁶ A rather different value for K_{hyd} can be derived from the forward and reverse rate constants for this process given in their Table 1, but the rate constants appear to have been extracted from Schöneshöfer et al. and marred by typographical errors. With the exclusion of the reports of Zhang and Field and of Schöneshöfer et al., the current study provides the first data bearing on the reversible hydrolysis of $(\text{SCN})_2$, K_{hyd} .

A variant of our proposed mechanism was suggested by Bjerrum and Kirschner,^{14,15} in which reaction M8 is replaced by



This alternative mechanism leads to the same stoichiometry, the same empirical rate law, and cannot be ruled out by our results. If this alternative were correct it would alter the derived rate law (eqs 18, 20) by replacing the factor of $3/2$ by the factor of 3, and corresponding adjustments would have to be made for the derived values of k_{disp} .

Our value of k_{disp} ($7 \times 10^4 \text{ M}^{-1} \text{ s}^{-1}$) might seem to conflict with the frequent reports of stable aqueous solutions of HOSCN and OSCN^- .^{9,20–22,62} Specifically, from data collected at pH 5–6 Thomas reported that HOSCN has a $\text{p}K_{\text{a}}$ of 5.3, that it undergoes second-order decomposition 20000-fold more slowly than we find, and that OSCN^- is essentially stable.⁶² An earlier paper by Aune and Thomas reported that HOSCN or OSCN^- decomposed with second-order kinetics and $k = 0.26 \text{ M}^{-1} \text{ s}^{-1}$ at $37 \text{ }^\circ\text{C}$ and pH 6.6;⁹ this result is consistent with Thomas's later result. Qualitatively similar results at pH 5–7.5 were reported by Hoogendorn et al.²⁰ Bjoerck and Claesson reported experiments that would have

(61) Moore, R. H.; Zeigler, R. K. *LSTSQR*; Los Alamos National Laboratory: Los Alamos, NM, 1959.

(62) Thomas, E. L. *Biochemistry* **1981**, *20*, 3273–3280.

required HOSCN/OSCN⁻ solutions to be stable for several hours at pH 6.7, and Thomas et al. have reported likewise.^{21,22} The apparent disagreement between these results and ours may be due to an unexplored pH-dependence in the HOSCN decomposition rate law, since our experiments were all performed at pH 2 or less.

By use of the temperature-dependent plot obtained in this work, rate constants can be calculated for comparison to earlier studies at different temperature values. A value of $k' = 0.0037 \text{ M}^3 \text{ s}^{-1}$ at 273 K can be inferred from our results, as compared to the value of $0.001 \text{ M}^3 \text{ s}^{-1}$ given by Stedman et al. at this temperature.¹ In the work of Figlar and Stanbury, a value of $0.093 \text{ M}^3 \text{ s}^{-1}$ is reported at 298 K,⁷ while our current results predict a value of $0.033 \text{ M}^3 \text{ s}^{-1}$ at this temperature. Finally, Bjerrum and Kirschner report a value of $0.076 \text{ M}^3 \text{ s}^{-1}$ at 291 K and at $\mu = 1.1$ and 1.2 M ,^{14,15} while our current results predict a value of $0.018 \text{ M}^3 \text{ s}^{-1}$ at this temperature. Thus, the values from the present work are a factor of 3.7 greater than that of Stedman, a factor of 4.1 smaller than that of Bjerrum and Kirschner, and a factor of 2.8 smaller than that of Figlar and Stanbury. Note that meaningful values of ΔH^\ddagger and ΔS^\ddagger cannot be derived from our data because we have not resolved values of k_{disp} as a function of temperature. Rather, the values plotted are calculated using the rate law observed by prior workers (eq 15) for comparison of the present results to those reported previously.

A second comparison with the work of Bjerrum and Kirschner relates to the rate dependence on $[\text{H}^+]$.^{14,15} In this early (1918) work, values of k' were observed to change significantly with changing $[\text{H}^+]$, with k' increasing by a factor of 1.65 with a change in $[\text{H}^+]$ from 1 M to 0.4 M. This should not be the case since their rate law containing k' explicitly takes into account the effect of acid concentration. However, in those experiments the ionic strength varied from 1.2 to 0.6 M, presumably because the concept of ionic strength had not yet been fully formulated. The ionic strength dependence obtained in the current work predicts that between $\mu = 0.5 \text{ M}$ and 1.2 M the value of k' shows a strong dependence on μ , with the value of k' decreasing with increasing μ (Figure 6). Thus, our data are in reasonable agreement with those collected by Bjerrum and Kirschner.^{14,15}

Thermochemical Analysis of Thiocyanogen Hydrolysis.

The following two equilibria have been reported in the literature:



The values reported for the equilibrium constants for these reactions are $K_{\text{ox}} = 3.7 \times 10^3 \text{ M}^{-1}$ ¹⁹ and $K_{\text{a}} = 5.0 \times 10^{-6} \text{ M}$.⁶² These equilibria can be combined to give the following:



It can be seen that $K_{\text{per}} = K_{\text{ox}}/K_{\text{a}}$. From the published values for K_{ox} and K_{a} , K_{per} is $7.4 \times 10^8 \text{ M}^{-2}$. This value can be used to calculate a free energy of formation of aqueous

Table 6. Calculated Enthalpies and Free Energies for Hypothetical Gas-Phase Reactions at 298 K

reaction	$\Delta H_{\text{rxn}}^\circ$, kJ/mol ^a	$\Delta G_{\text{rxn}}^\circ$, kJ/mol ^a
$(\text{SCN})_2 + \text{Cl}_2 \rightleftharpoons (\text{SCl})_2 + (\text{CN})_2$	-91.4	-89.8
$(\text{SCN})_2 + 2\text{Cl}_2 \rightleftharpoons (\text{SCl})_2 + 2\text{ClCN}$	-136.8	-137.7
$(\text{SCN})_2 + 2\text{CH}_4 \rightleftharpoons (\text{SCH}_3)_2 + 2\text{HCN}$	13.2	8.7
$(\text{SCN})_2 + \text{C}_2\text{H}_6 \rightleftharpoons (\text{SCH}_3)_2 + (\text{CN})_2$	-7.4	-6.4
$(\text{SCN})_2 + 2\text{C}_2\text{H}_6 \rightleftharpoons (\text{SCH}_3)_2 + 2\text{CH}_3\text{CN}$	-80.7	-84.9
$2\text{HOSCN} + 2\text{Cl}_2 \rightleftharpoons (\text{SCl})_2 + (\text{CN})_2 + 2\text{HOCl}$	30.5	27.2
$2\text{HOSCN} + \text{Cl}_2 \rightleftharpoons (\text{SCl})_2 + (\text{CN})_2 + \text{H}_2\text{O}_2$	48.9	52.1
$2\text{HOSCN} + 2\text{CH}_4 \rightleftharpoons (\text{SCH}_3)_2 + (\text{CN})_2 + 2\text{H}_2\text{O}$	-149.9	-148.8
$2\text{HOSCN} + \text{C}_2\text{H}_6 \rightleftharpoons (\text{SCH}_3)_2 + (\text{CN})_2 + \text{H}_2\text{O}_2$	132.8	135.5

^a Values calculated from the ΔH and ΔG values given in Table S-13.

HOSCN, ΔG_f° (HOSCN(aq)), using the following equations and ΔG_f° values from the NBS tables of chemical thermodynamic values:⁶³

$$\Delta G_{\text{per}}^\circ = -RT \ln(K_{\text{per}}) \quad (25)$$

$$\Delta G_{\text{per}}^\circ = \Delta G_f^\circ(\text{HOSCN(aq)}) + \Delta G_f^\circ(\text{H}_2\text{O(l)}) - \Delta G_f^\circ(\text{H}_2\text{O}_2(\text{aq})) - \Delta G_f^\circ(\text{H}^+(\text{aq})) - \Delta G_f^\circ(\text{SCN}^-(\text{aq})) \quad (26)$$

From these equations, ΔG_f° (HOSCN(aq)) is 145 kJ/mol.

A similar analysis was performed on the $(\text{SCN})_2$ hydrolysis equilibrium shown in step M6 of Table 4 using our experimental value for K_{hyd} , ΔG_f° (HOSCN(aq)) from the above analysis, and ΔG_f° for the remaining species from the NBS tables. Using such an analysis, ΔG_f° ((SCN)₂(aq)) is calculated to be 456 kJ/mol.

This value can be used to derive the free energy of solvation of $(\text{SCN})_2$ from the experimental enthalpy of formation of $(\text{SCN})_2(\text{g})$ reported by Vanderzee and Quist: ΔH_f° ((SCN)₂(g)) = 344 kJ/mol.⁶⁴ On the basis of entropy values reported in the NBS tables for molecules of similar size, the value of S° ((SCN)₂(g)) can be estimated to be 300 (± 50) J/(mol K). Using this value, entropy values for the elements as reported in the NBS tables,⁶³ and the value of ΔH_f° ((SCN)₂(g)) from Vanderzee and Quist, ΔG_f° ((SCN)₂(g)) is 334 (± 15) kJ/mol at 298 K. This value, taken with the value calculated for ΔG_f° ((SCN)₂(aq)) above, implies that the free energy of solvation of $(\text{SCN})_2$ is highly unfavorable: $\Delta G_{\text{sol}}^\circ$ ((SCN)₂) = 122 kJ/mol. This value is unreasonably large as compared to the values for the halogens: $\Delta G_{\text{sol}}^\circ(\text{X}_2) = 6.94 \text{ kJ/mol}$, 0.82 kJ/mol , and -2.93 kJ/mol for X = Cl, Br, and I, respectively.⁶³ This unexpectedly large value for $\Delta G_{\text{sol}}^\circ$ ((SCN)₂) prompted a high-level computational quantum study aimed at identifying the source of the disagreement.

Using *Gaussian 98*, DFT calculations were performed at the G3B3 level on all of the species in the hypothetical gas-phase reactions shown in Table 6.⁴² The geometries of these species were optimized in this calculation at the B3LYP/6-31G(d) level (Tables S-7 to S-12, Supporting Information).⁴³ Vibrations were then calculated at the same level, yielding

(63) Wagman, D. D.; Evans, W. H.; Parker, V. B.; Schumm, R. H.; Halow, I.; Bailey, S. M.; Churney, K. L.; Nuttall, R. L. *J. Phys. Chem. Ref. Data* **1982**, *11*, Suppl. No. 2.

(64) Vanderzee, C. E.; Quist, A. S. *Inorg. Chem.* **1966**, *5*, 1238–1242.

the total enthalpies and free energies listed in Table S-13 (Supporting Information). Gaseous free energies and enthalpies of reaction were calculated from these quantities and are listed in Table 6. Free energies of solvation ($\Delta G_{\text{sol}}^\circ$) were calculated at the CPCM/B3LYP/6-311+G(2d,p)//B3LYP/6-31G(d) level, and are listed in Table S-13.

From the first five derived enthalpies of reaction listed in Table 6, ΔH_f° values can be calculated for gaseous $(\text{SCN})_2$ using Hess's law calculations and the gas-phase values of ΔH_f° reported in the NBS tables for the other species in these equilibria.⁶³ From these reactions, it is calculated that $\Delta H_f^\circ((\text{SCN})_2(g)) = 378 \pm 14$ kJ/mol. This calculated value of $\Delta H_f^\circ((\text{SCN})_2(g))$ is quite different from the experimental value (344 kJ/mol).⁶⁴ It is unclear whether this difference is the result of some aspect of the computational technique used or difficulties in the experimental determination. However, due to the consistency of the results obtained from several different reactions, the computational result appears to be of adequate quality for the calculation of these parameters. Similarly, by combining the gaseous free energy changes in Table 6 with NBS data, the value of $\Delta G_f^\circ((\text{SCN})_2(g))$ is calculated to be 353 ± 14 kJ/mol. This result, when combined with the value for $\Delta G_f^\circ((\text{SCN})_2(aq))$ derived from the values published for K_{ox} and K_a , yields an unreasonably large value of 103 kJ/mol for $\Delta G_{\text{sol}}^\circ((\text{SCN})_2)$. Note also that the solvation free energy for $(\text{SCN})_2$ calculated by the CPCM/DFT method is -14.3 kJ/mol, which provides further evidence that a solvation energy of 103 kJ/mol is unreasonable. These considerations imply that there is a substantial error in the value of $\Delta G_f^\circ((\text{SCN})_2(aq))$ derived from the values published for K_{ox} and K_a .

A similar analysis can be performed on the last four reactions listed in Table 6 for the determination of ΔG_f° for gaseous and hydrated HOSCN. Using a set of calculations similar to those discussed above, it is calculated that, at $T = 298$ K, $\Delta G_f^\circ(\text{HOSCN}(g)) = 53.0 \pm 0.7$ kJ/mol. With the solvation free energy of -34.4 kJ/mol listed in Table S-13 for HOSCN, $\Delta G_f^\circ(\text{HOSCN}(aq))$ is 18.6 kJ/mol. Using this value in eq 26, $\Delta G_{\text{per}}^\circ$ is -177 kJ/mol. From this value of $\Delta G_{\text{per}}^\circ$, it can be calculated that $K_{\text{per}} = K_{\text{ox}}/K_a = 1.13 \times 10^{31} \text{ M}^{-2}$, as compared to the value of $7.4 \times 10^8 \text{ M}^{-2}$ from the published values for K_{ox} and K_a .^{19,62} For the published values of K_{ox} and K_a , $\Delta G_{\text{per}}^\circ = -50.6$ kJ/mol. Clearly, there is a major disagreement between these values, further indicating that either the published value for K_{ox} or the published value for K_a is in error.

Using the solvation energies calculated for $(\text{SCN})_2$ and HOSCN, a calculation can be performed for the hydrolysis equilibrium seen in step M6 of the mechanism in Table 4. Using an equation similar to the one shown in eq 26, the values of $\Delta G_f^\circ(\text{HOSCN}(aq))$ and $\Delta G_f^\circ((\text{SCN})_2(aq))$ from the above DFT calculations, and the relevant values from the NBS tables, it can be calculated that $\Delta G_{\text{hyd}}^\circ$ is 9.4 kJ/mol for the reaction shown in step 6 of the proposed mechanism.⁶³ From the experimental value of K_{hyd} derived from the ϵ_{eff} and k_{obs} data in the present work, $\Delta G_{\text{hyd}}^\circ$ is 18.6 kJ/mol. This computational result indicates that the currently obtained experimental value for K_{hyd} is reasonable and that the

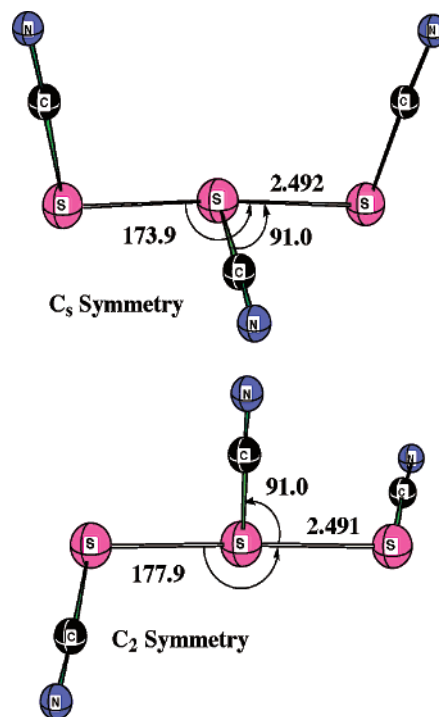


Figure 8. $(\text{SCN})_3^-$ geometries optimized at the B3LYP/6-311+G(2d) level using *Gaussian 98*.

Table 7. Calculated Total Enthalpies and Free Energies and Free Energies of Hydration at 298 K for Species Involved in Step M5 of the Proposed Mechanism^a

species	ΔH , au ^b	ΔG , au ^b	$\Delta G_{\text{sol}}^\circ$, kJ/mol ^c
SCN^-	-490.559151	-490.585643	-239.4
$(\text{SCN})_2$	-980.929827	-980.969233	-14.3
$(\text{SCN})_3^-$ ^d	-1471.529720	-1471.584047	-148.0
$(\text{SCN})_3^-$ ^e	-1471.531218	-1471.584757	-145.7

^a All values were calculated using *Gaussian 98*. ^b Values calculated at the G3MP2B3 level at 298 K. ^c Solvation energies calculated at the CPCM/B3LYP/6-311+G(2d,p)//B3LYP/6-31G(d) level at 298 K. ^d C_s isomer of $(\text{SCN})_3^-$. ^e C_2 isomer of $(\text{SCN})_3^-$.

literature value for K_{ox} is, most likely, far from correct.¹⁹ Also, this calculated value is incompatible with the value of $\Delta G_{\text{hyd}}^\circ = 70$ kJ/mol derived from the value of K_{hyd} in the work of Schöneshöfer et al.¹⁶ This lack of agreement indicates that the value of K_{hyd} determined in the work of Schöneshöfer et al. is incorrect.

Theoretical Calculation of $K_{(\text{SCN})_3^-}$. A set of ab initio calculations was performed on each of two possible geometries of $(\text{SCN})_3^-$.⁴² The geometries resulting from these calculations can be seen in Figure 8. Both of these isomers were stable, and the enthalpy (298 K) difference between the two was found to be only 3.9 kJ/mol. Note that these geometries are different from those calculated at the PM3/DN** level earlier in this laboratory.²⁹ The currently calculated molecules are both T-shaped about the central sulfur atom, in agreement with the predictions of VSEPR theory. The pseudo trigonal planar geometries obtained previously using the PM3/DN** method appear to be artifacts of that method.²⁹

Calculations were performed at the G3MP2B3 level on the three species involved in the association of SCN^- with $(\text{SCN})_2$ to form $(\text{SCN})_3^-$ (reaction M5).⁴³ The results of these

calculations are given in Table 7. Values of the free energy change for this reaction, $\Delta G_{\text{scn}}^{\circ}$, can be calculated using the following equation:

$$\Delta G_{\text{scn}}^{\circ} = \Delta G((\text{SCN})_3^-(g)) + \Delta G_{\text{sol}}((\text{SCN})_3^-) - \Delta G(\text{SCN}^-(g)) - \Delta G_{\text{sol}}(\text{SCN}^-) - \Delta G((\text{SCN})_2(g)) - \Delta G_{\text{sol}}((\text{SCN})_2) + \text{correction} \quad (27)$$

The correction noted in this equation is for the phase change from the gas phase (1 mol/24.27 L) to the solution phase (1 mol/L).^{46,47} This correction is 7.95 kJ/mol for each species in the reaction, which leads to a net correction of -7.95 kJ/mol. From this equation, $\Delta G_{\text{scn}}^{\circ} = 21.3$ kJ/mol for this reaction. From the value of $0.43 \pm 0.29 \text{ M}^{-1}$ used for $K_{(\text{SCN})_3^-}$ in the current work, a value of 2.27 kJ/mol is calculated for $\Delta G_{\text{scn}}^{\circ}$. The difference between the theoretical value⁶⁵ and the experimentally derived value is not unexpected, due to the large uncertainty associated with $K_{(\text{SCN})_3^-}$ and to the large uncertainty expected in the calculation of ΔG_{sol} of ions.

(65) The calculated G3MP2B3 equilibrium free energy $\Delta G_{\text{scn}}^{\circ}$ is reduced to 18.3 kJ/mol when geometries are computed at the CPCM/B3LYP/6-31+G(d) level rather than B3LYP/6-31G(d). At the CPCM/B3LYP/6-31+G(D) level the C_2 minimum for $(\text{SCN})_3^-$ distorts slightly to C_1 symmetry. The latter geometry (C_1) was used for the G3MP2B3 and solvation calculation.

(66) Awtrey, A. D.; Connick, R. E. *J. Am. Chem. Soc.* **1951**, *73*, 1842–1843.

(67) Buckles, R. E.; Mills, J. F. *J. Am. Chem. Soc.* **1953**, *75*, 552–555.

(68) Liu, Q.; Margerum, D. W. *Environ. Sci. Technol.* **2001**, *35*, 1127–1133.

(69) Zimmerman, G.; Strong, F. C. *J. Am. Chem. Soc.* **1957**, *79*, 2063–2066.

(70) Beckwith, R. C.; Wang, T. W.; Margerum, D. W. *Inorg. Chem.* **1996**, *35*, 995–1000.

(71) Palmer, D. A.; van Eldik, R. *Inorg. Chem.* **1986**, *25*, 928–931.

Conclusion

The reaction of aqueous chlorine with excess SCN^- at pH 2–0 is a convenient in situ method for the preparation of thiocyanogen solutions. These solutions consist of a mixture of $(\text{SCN})_2$, $(\text{SCN})_3^-$, and HOSCN, which are interconverted through two simultaneous equilibria: $K_{(\text{SCN})_3^-}$ ($= 0.43 \pm 0.29 \text{ M}^{-1}$) and K_{hyd} ($= (5.66 \pm 0.77) \times 10^{-4} \text{ M}^2$). The solutions decompose through a complex rate law (eq 18a) that can be derived from the assumption that the second-order disproportionation of HOSCN is rate limiting ($k_{\text{disp}} = 7 \times 10^4 \text{ M}^{-1} \text{ s}^{-1}$).

These results give good support and extra detail for some prior reports on the chemistry of thiocyanogen while refuting others. The large body of reports from the biochemical literature indicating considerable stability for HOSCN/OSCN⁻ at physiological pH suggests the need for further study to explain the transition from the rapid decomposition we find at low pH.

Acknowledgment. The authors thank the NSF for funding this research. This material is based upon work supported by the National Science Foundation under Grant No. 0138142. Any opinions, findings, and conclusions or recommendations expressed in this material are those of the author(s) and do not necessarily reflect the views of the National Science Foundation. Professor Doug Goodwin (Auburn) is thanked for the use of his Applied Photophysics stopped-flow instrument.

Supporting Information Available: Tables showing the instrument dependence of A_0 , the ion-chromatography retention times, the values of k_{obs} , the standard geometries used in the DFT calculations, and the DFT energies. Derivations of eqs 19 and 20. This material is available free of charge via the Internet at <http://pubs.acs.org>.

IC049356S